

High Spin Spectroscopy for $A \approx 160$ Nuclei

CONF-8909247--4

C.-H. Yu

DE90 007058

*The Niels Bohr Institute, University of Copenhagen
Blegdamsvej 17, Copenhagen O, Denmark
and*

*Dept. of Physics and Astronomy
The University of Tennessee
Knoxville TN. 37966-1200, U.S.A.*

J. Gascon*, J.D. Garrett†, and G.B. Hagemann

*The Niels Bohr Institute, University of Copenhagen
Blegdamsvej 17, Copenhagen O, Denmark*

Abstract

Experimental routhians, alignments, band crossing frequencies, and the $B(M1)/B(E2)$ ratios of the $N = 90$ isotones and several light Lu ($N = 90 - 96$) isotopes are summarized and discussed in terms of shape changes. These systematic analyses show a neutron and proton number dependent deformations (both quadruple and γ deformations) for these light rare earth nuclei. The stability of the nuclear deformation with respect to β and γ is also found to be particle number dependent. Such particle number dependent shapes can be attributed to the different locations of the proton and neutron Fermi levels in the Nilsson diagrams. Configuration dependent shapes are discussed specially concerning the deformation difference between the proton $h_{9/2} \frac{1}{2}^- [541]$ and the high-K $h_{11/2}$ configurations. The observed large neutron band crossing frequencies in the $h_{9/2} \frac{1}{2}^- [541]$ configuration support the predicted large deformation of this configuration; but can not be reproduced by the cranked shell model calculation according to the predicted deformations. Lifetime measurement for ^{157}Ho , one of the nuclei that show such a large $\hbar\omega_c$ in the $\frac{1}{2}^- [541]$ band, indicates that deformation difference can only account for 20% of such shift in $\hbar\omega_c$.

*Present address: Laboratoire de Physique Nucléaire, C.P. 612, Succ "A", Université de Montréal, Montréal, Québec H3C - 3J7, Canada

†Present address: Oak Ridge National Laboratory, Oak Ridge, Tennessee 37831, U.S.A.

1. Introduction

Large amount of experimental data and theoretical interpretations exists for the near-yrast spectroscopy at high angular momentum in the rare-earth region. Most of these investigations, however, have been concentrated on the study of even-even and odd- N nuclei, for example, the series of ytterbium nuclei ([Gaa.1], [Jön.2], [Kow.1], [Rie.1], [Roy.1] and [Wal.1]). Such studies have provided a understanding of many high spin phenomena, such as rotational band crossings due to the alignment of pairs of quasineutrons and quasiprotons; the quenching of static neutron pair correlations at high angular momentum; the dependence of the nuclear shape on particle number, configuration and rotational frequency, etc.

It is important to extend such high spin studies to odd- Z nuclei in order to establish the spectrum of proton states at large angular momentum. Many phenomena, for example, the variation of the nuclear shape induced by the occupation of various single-proton orbitals with different deformation driving forces, can be studied and compared with the corresponding neutron effect. Furthermore, because of the large g -factors associated with an unpaired proton, it is possible to investigate the details of the nuclear wave functions by studying the magnetic dipole transition probabilities between the favoured and unfavoured signature sequences of specific configurations.

A series of experiments have been carried out recently to study the odd- Z light rare earth nuclei, e.g, ^{161}Lu ([Yu.1]), ^{165}Lu ([Jön.1], [Fra.1], [Fra.2]), ^{167}Lu ([Yu.2]), and ^{157}Ho ([Gas.2]). Together with the existing data for another odd- A lutetium isotopes, ^{163}Lu ([Hon.1]), and the odd- Z , $N = 90$ isotones, $^{159}\text{Tm}_{90}$ ([Lar.1], [Lar.2], [Sim.1], and [Gas.1]) and $^{157}\text{Ho}_{90}$ ([Hag.1], [Sim.2] and [Rad.1]) the newly measured data make the odd- A lutetium isotopes and the $N = 90$ isotones the best studied odd- Z isotopic and isotonic chain at high spin. A systematic analysis on these isotopes and isotones can therefore be made for specific configurations.

The spectroscopy for quasiproton configurations would be identical for all the lutetium isotopes in the absence of mean field changes, since the proton configurations are the same for all the isotopes. Changes of the single proton state spectrum as a function of the neutron number will be particularly sensitive to changes in the nuclear shape. This sensitivity combined with the variety of proton orbitals (both down- and up-spinning orbitals on the Nilsson diagrams) in this mass region leads to a very

detailed and interesting spectroscopy for these nuclei. The heaviest lutetium isotope, $^{167}\text{Lu}_{96}$, is the most stably deformed nucleus presented in this work. The rotational effect on single proton motion is exhibited in this nucleus with the least ambiguity. As a result this nucleus sets a benchmark for such a study in a stably deformed system. With the decrease of neutron number, both the magnitude and stability of the nuclear deformation is expected to decrease. The lightest lutetium isotope, $^{161}\text{Lu}_{90}$, is near to the transitional region where the nuclear deformation changes from prolate to spherical shape. Consequently it is least stable with respect to deformations. In such a “soft” system, the configuration- and angular momentum-dependent nuclear shapes are expected. The rotational modification on single proton motion in a “soft” system can also be investigated and compared with the more stably deformed system.

Combined with the data of even-even, $N = 90$ isotones, ^{162}Hf ([Hüb.1], ^{160}Yb ([Rie.1] and [Gaa.1]) and ^{158}Er ([Sim.4] and [Tjø.1]), the odd- Z , $N = 90$ isotones make the $N = 90$ isotonic chain the best studied isotonic chain at high spin. A systematic study of these isotones allows the investigation of nuclear shapes influenced by the changing mean field due to the change of proton Fermi surface.

Figure 1 is a map of the nuclei to be discussed. The contrasting locations of proton and neutron Fermi levels on the Nilsson diagrams (see fig.2) for these two chains of nuclei (in the upper- and lower- portions of the shell respectively) make the comparison of isotopic and isotonic systematics most sensitive to the configuration and particle number dependent shapes.

2. Systematic Trend of Deformations at Low Angular Momentum

2.1 Energy Signature Dependence at Low Spin

Energy signature splittings are observed at low angular momentum for the odd-mass lutetium isotopes and $N = 90$ isotones, see fig.3. This figure summarizes the energy signature splitting, $\Delta\epsilon'$, as a function of rotational frequency for ^{157}Ho , $^{159}\text{Tm}_{90}$, and $^{161-167}\text{Lu}_{90-96}$. $\Delta\epsilon'$ is defined as

$$\Delta\epsilon' = \epsilon'(-, +\frac{1}{2}) - \epsilon'(-, -\frac{1}{2}), \quad (1)$$

where the parameters inside the parentheses are parity and signature, (π, α) , and ϵ' is the experimental routhian for the corresponding configurations. The dramatic

feature shown in fig. 3 is the particle number dependence of the magnitude of the signature splittings at $\hbar\omega < \hbar\omega_c$. The splittings are most dramatic for the lighter lutetium isotopes (e.g. ^{161}Lu and ^{163}Lu). For the $N = 90$ isotones, the splittings are pronounced for all the three nuclei with the heaviest isotone, ^{161}Lu , having the largest $\Delta\epsilon'$. Such a large splitting at low spin for these nuclei is difficult to understand if axially symmetric shapes are assumed. For axially symmetric nuclei, a signature dependent decoupling in energy is expected and observed in the $K = \frac{1}{2}$ rotational sequences. The signature dependent term in the hamiltonian has different signs for the $\alpha = +\frac{1}{2}$ and $-\frac{1}{2}$ sequences thus producing the decoupled energies for the $K = \frac{1}{2}$ decay sequences. In a deformed rotating system, K is not a conserved quantum number. The Coriolis interaction, which mixes $K = \frac{1}{2}$ components into the wave function of bands with $K \neq \frac{1}{2}$, leads to signature splitting in sequences with $K \neq \frac{1}{2}$. Such a splitting depends on the magnitude of the Coriolis matrix elements, which in first order connect states with $\Delta K = \frac{1}{2}$ ([Boh.1]). Therefore the splitting for configurations with very large K is inhibited at low spin. The decay sequences shown in fig. 3 are associated with the orbits in the middle or upper portion of the $h_{11/2}$ "high- j intruder" proton subshell. These orbits (either the $\frac{9}{2}^- [514]$ or the $\frac{7}{2}^- [523]$ Nilsson configuration) have large K values at $\hbar\omega = 0$ ($K = 9/2$ or $7/2$). The rotational frequency at which the large splitting occurs is not high enough to allow sufficient admixture of the low- K components into the wave function. Thus large signature splitting is not expected. Indeed, a simple cranked shell model calculation assuming axially symmetric shapes predicts no signature splitting in energy for $\hbar\omega < 0.25\text{MeV}$. The large signature splittings for these isotones at low spin can be understood ([Ben.1], [Fra.3], [Lea.1], and [Yu.1]) as the deviation of the nuclear shapes from axial symmetry (i.e. γ -deformation). The occupation of a high- j quasiproton with the favoured signature (the $\alpha = -1/2$ signature for $h_{11/2}$ shell) strongly polarizes the core shape especially in γ degree of freedom. The nuclear shape is "driven" toward $\gamma > 0$ for λ in the lower portion of the shell, not affected for λ in mid-shell and "driven" toward $\gamma < 0$ for λ in the upper portion of the shell (Lund convention, see ref. [And.1]). In contrast, the polarization effect of occupying a quasiproton with the unfavoured signature is small. The predicted dependence of the two signatures of the lowest negative-parity quasiproton configurations on γ deformation is shown for $Z \approx 71$ in fig.4. This figure

shows that both signature components of the lowest $h_{11/2}$ protons are energetically favoured at negative γ values. The $\alpha = -\frac{1}{2}$ orbit lies lower in energy and has a pronounced minimum at a rather large negative value of γ . Such a non-axially symmetric shape of the nucleus and the different shapes of the two signatures give an enhanced energy signature splitting compared to the axially symmetric system.

Not only can the signature partners of soft nuclei assume different γ deformations, but such signature-dependant γ deformations will change as a function of the proton and neutron numbers. The nucleus is either driven toward different γ deformations or not influenced by the valence particles depending on the relative positions of the Fermi levels in the shell (see the preceding paragraph). Indeed, the increase of energy signature splitting in the negative-parity decay sequences of the $N = 90$ isotones with increasing Z is attributed to such a change in the γ deformation between the middle and the upper portion of the $h_{11/2}$ shell. For example, a static γ deformation of about -20° is necessary to account for the observed splitting of the negative-parity configurations in $^{161}\text{Lu}_{90}$ below the band crossing, and those for $^{159}\text{Tm}_{90}$ and $^{157}\text{Ho}_{90}$ are -16° and -10° respectively ([Ham.1]). It, however, is difficult to distinguish the effect of a static γ deformation from a softness in the γ degree of freedom.

The changing of the proton Fermi level also affects the β_2 deformation of the nucleus. This can be qualitatively understood from the proton Nilsson diagrams, see fig. 2. The occupation of an oblate proton orbit* drives the nucleus toward a smaller quadruple deformation. Such a decrease of quadruple deformation also gives rise to increased signature splitting since the proton Fermi level is closer to the low- K components of the shell for smaller quadruple deformations.

The neutron number dependence of changes in the spectra of quasiproton states for an odd- Z isotopic chain particularly reflects changes in the nuclear shape, since to first approximation the same spectra are expected for identical quasiproton configurations assuming the same shape. Differences in the spectra of quasiproton states therefore are directly attributed to different nuclear shapes. In fig.3 the drastic decrease of energy signature splitting at low spin with increasing neutron number for

* The definition of prolate and oblate orbitals, downward and upward sloping respectively, on the Nilsson diagrams, see fig.5, distinguishes the relative projection of the intrinsic angular momentum on the nuclear-symmetry and rotational axes. Oblate and prolate orbitals are illustrated for a prolate nucleus in fig.5

the lutetium isotopes is a clear indication of shape changes from the lighter to heavier isotopes. The decrease of splitting with increasing neutron number is the result of both the increased stability of the axially symmetric shapes and the increased magnitude of the quadruple deformation associated with the occupation of downward sloping neutron Nilsson levels between $N = 90$ and 96 , see the right-hand side of fig. 2. In contrast to the case of protons as discussed in the preceding paragraphs, the occupation of prolate neutron orbitals at the lower portion of the $\nu i_{13/2}$ shell drives the nucleus toward positive γ and larger quadruple deformations. The almost vanishing energy signature splitting in ^{167}Lu indicates that this nucleus is most stably deformed and has the largest quadruple deformation and the least deviation from axial symmetry.

Self-consistent calculations ([Wys.1]) also show consistent deformation systematics for these isotopes. Fig. 6 shows the the $\beta_2 - \gamma$ dependence of the total routhians for the lowest negative-parity, $\alpha = -1/2$ configurations in the odd-mass $N = 90$ and $Z = 71$ nuclei at $\hbar\omega \approx 0.2$ MeV. Such plots show a particle number dependence of the stability of the nuclear shapes. The total routhian minimum is best defined on the β_2 - γ plane for the heaviest lutetium isotope, ^{167}Lu . This nucleus has also the largest quadruple deformation and the smallest deviation from axial symmetry (the energy minimum has the largest β_2 and $\gamma \approx 0$). With the decrease of neutron number the stability of the nuclear deformation decreases, i.e. the energy minimum becomes less well defined with respect to β_2 and γ . This "softness" is especially pronounced with respect to γ . For $^{161}\text{Lu}_{90}$, the lowest energy contour line has γ values varying from $< -30^\circ$ to $+10^\circ$. The quadruple deformation is also significantly reduced from $N = 96$ to 90 . For the $N = 90$ isotones, the removal of the upper-shell $h_{11/2}$ protons by decreasing the proton number from 71 to 67 apparently stabilizes the nuclear shape especially with respect to γ and increases the quadruple deformation β_2 . Such a systematics is in agreement with the observed systematic trend of the energy signature dependence.

2.2 Signature Dependence of Transition Rates at Low Spin

The large energy signature splitting discussed in the preceding subsection is a clear indication of non-axially symmetric shapes for the lighter lutetium isotopes and $N = 90$ isotones, but not a definite evidence. Since different models based on dif-

ferent assumptions and parameters predict different magnitudes of energy splittings even for the same deformation, it is important to investigate additional experimental quantities that are sensitive to the deformations.

Figure 7 shows the relative ratios, $B(M1, I \rightarrow I - 1)/B(E2, I \rightarrow I - 2)$, of the reduced magnetic dipole and electric quadrupole transition probabilities of the decay sequences associated with the lowest $\pi h_{11/2}$ configurations for $^{157}\text{Ho}_{90}$, $^{159}\text{Tm}_{90}$ and $^{161-167}\text{Lu}_{90-96}$. In fig.7, the $B(M1, I \rightarrow I - 1)/B(E2, I \rightarrow I - 2)$ ratios at low spin (below the first band crossing) are characterized by a signature dependence that is smallest for the heaviest lutetium isotope, ^{167}Lu . Lifetime measurements for $^{157}\text{Ho}_{90}$ ([Hag.1]) and $^{159}\text{Tm}_{90}$ ([Gas.1]) show no signature dependence of $B(E2, I \rightarrow I - 2)$ values at low spin within the experimental uncertainties of 20% and 15% for $^{159}\text{Tm}_{90}$ and $^{157}\text{Ho}_{90}$ respectively. The observed signature dependence of the $B(M1)/B(E2)$ ratios is therefore attributed to the $B(M1, I \rightarrow I - 1)$ values.

The signature dependence of $B(M1)$ values is related to the amplitude of $K = \frac{1}{2}$ component in the wave function through a mechanism similar to the decoupling in the excitation energies responsible for the energy signature splitting discussed in the preceding subsection. Such a signature dependence of $B(M1)$ values does not in itself give definite evidence for the triaxiality of the nuclear shape. However, it is proved ([Hag.3]) that there exists a definite relation between the signature splittings of routhians and the $B(M1)$ values, if the nucleus has an axially symmetric shape. In a semiclassical approximation ([Dön.1]) based on cranking, if the nucleus is axially symmetric about the z -axis or has a very small triaxiality, the reduced M1-transition probability is:

$$B(M1, I \rightarrow I - 1) = \frac{3}{8\pi} K^2(\omega) \{ (g_p - g_R) \left[\sqrt{1 - \frac{K(\omega)^2}{I^2}} - \frac{i_n}{I} \pm \frac{\Delta e'}{h\omega} \right] - (g_n - g_R) \frac{i_n}{I} \}^2 \quad (2)$$

Therefore below the band crossing (i.e. $i_n = 0$).

$$\frac{B(M1, \alpha = +\frac{1}{2} I \rightarrow \alpha = -\frac{1}{2} I - 1)}{B(M1, \alpha = -\frac{1}{2} I \rightarrow \alpha = +\frac{1}{2} I - 1)} = \frac{\sqrt{1 - \frac{K(\omega)^2}{I^2}} - \frac{i_n}{I} + \frac{\Delta e'}{h\omega}}{\sqrt{1 - \frac{K(\omega)^2}{I^2}} - \frac{i_n}{I} - \frac{\Delta e'}{h\omega}} \quad (3)$$

Particle-rotor calculations ([Hag.3]) also show that a similar relation is valid for axially symmetric shapes, and that it works very well in the deformation-aligned limit. The validity of this relation is therefore a test of the axial symmetry of the

nuclear shape. From eq. (3) the relative signature dependence of $B(M1)$ values can be expressed by:

$$\frac{\Delta B(M1)}{B(M1)_{\text{axt}}} = \frac{4X \frac{\Delta \epsilon'}{h\omega}}{X^2 + (\frac{\Delta \epsilon'}{h\omega})^2} \quad (4)$$

where $X = \sqrt{1 - \frac{k^2(\omega)}{I^2}} - \frac{i_p}{I}$.

The relative splitting $\frac{\Delta B(M1)}{B(M1)_{\text{axt}}}$ can be extracted from experimental $B(M1)/B(E2)$ ratios, and compared to the empirical values calculated from the right hand side of eq. (4) using experimental values of $\Delta \epsilon'/h\omega$. The results of both experimental and empirical values of $\Delta B(M1)/B(M1)$ are shown in fig.8 for $^{157}\text{Ho}_{90}$, $^{159}\text{Tm}_{90}$, and $^{161-167}\text{Lu}_{90-96}$ at spin $I \approx 10$. The "expected" $\Delta B(M1)/B(M1)_{\text{axt}}$ values are overestimated for ^{157}Ho and ^{165}Lu by more than a factor of two and for ^{159}Tm , $^{161,163}\text{Lu}$ by a factor of 3 -4. For ^{167}Lu the expected value is close to the experimental value. The large discrepancies between the expected and measured values for ^{161}Lu , ^{163}Lu , and ^{159}Tm suggest sizable triaxial deformations for these nuclei. This conclusion is consistent with the large energy signature splittings at this spin region discussed in the preceding subsection.

3. Deformation and the AB Neutron Band Crossings

One of the indirect informations about the nuclear deformation is the band crossing frequency, $h\omega_c$, which in many cases can be determined accurately from experiment. Theoretically such a crossing frequency is associated with: (1) the projection, j_x , of the angular momentum component on the rotation axis for the aligning orbitals responsible for the band crossing; and (2) the quasiparticle energies of the aligning orbitals defined as:

$$E_\nu = \sqrt{\Delta^2 + (\epsilon_\nu - \lambda)^2} \quad (5)$$

where Δ , ϵ_ν and λ are the pair gap parameter, the single particle energy of state ν and the Fermi level associated with the appropriate particle number. For nuclei with Fermi levels close to the aligning orbits [therefore $(\epsilon_\nu - \lambda)$ is small in eq. (5)], band crossing frequencies are dominantly determined by pair gap, Δ . Band crossing frequencies are also sensitive to the relative position of the Fermi level with respect to the aligning orbitals. This influence is specially important when the single particle term, $(\epsilon_\nu - \lambda)^2$, in eq. (5) is large. Thus deformation can influence $h\omega_c$ by changing the position of Fermi level relative to the aligning orbitals.

In the past few years, studies on some Ta and Re isotopes ([Bac.1], [Wal.2]) have shown that the AB neutron band crossing is shifted to a larger frequency in the proton $h_{9/2} \frac{1}{2}^- [541]$ Nilsson configuration relative to the other configurations. Such shifts of the AB neutron band crossing frequencies are also observed in some light rare earth nuclei, e.g. ^{167}Lu ([Yu.2]), ^{165}Lu ([Jön.1]) and ^{157}Ho ([Rad.1]). The magnitudes of these shifts, measured relative to the average crossing frequency in the yrast sequences of the neighbouring even-even isotones:

$$\delta\hbar\omega_c = \hbar\omega_c(\text{odd} - Z, \frac{1}{2}^- [541]) - \hbar\omega_c(\text{even} - \text{even}, \text{yrast}), \quad (6)$$

are summarized in fig. 9. Deformation effects qualitatively describe ([Wal.2]) the shift of $\hbar\omega_c$ to larger frequencies in the $\frac{1}{2}^- [541]$ configuration. The strongly down-sloping $\frac{1}{2}^- [541]$ orbit in the Nilsson diagrams (see the left-hand side of fig. 2) drives the nuclear shapes toward a large quadruple deformation. As a result, the nuclear deformation is larger when an odd proton occupies this orbit compared to the occupation of other orbits. Indeed, self-consistent cranking calculations reproduce ([Wal.2]) most of the observed shift for $^{177}\text{Re}_{102}$. It should be noted, however, that not only is the observed $\hbar\omega_c$ relatively small in $^{177}\text{Re}_{102}$ (e.g. less than half of that in $^{167}\text{Lu}_{96}$, see fig. 9), but also the $i_{13/2}$ quasineutron band crossing for this nucleus, for which the Fermi level is moved away from the highly alignable orbits, is more sensitive to the deformation. This sensitivity decreases with the decreasing neutron number. For the 96 neutrons of $^{167}\text{Lu}_{96}$, the neutron Fermi level is closer to the highly alignable $i_{13/2}$ orbitals than for $^{177}\text{Re}_{102}$. Therefore the quasineutron energy, E_ν , is less sensitive to deformation changes. Self-consistent calculations ([Naz.1]) based on a Woods-Saxon nuclear potential only predict about 50% of the observed shift in crossing frequencies for the $\frac{1}{2}^- [541]$ decay sequence in ^{167}Lu . For the lightest nuclei shown in fig. 9, $^{157}\text{Ho}_{30}$, the predicted shift is less than 20% of the observed value. A recent measurement ([Gas.2]) of the lifetimes for both the $h_{9/2} \frac{1}{2}^- [541]$ and the $h_{11/2} \frac{5}{2}^- [523]$ configurations in ^{157}Ho indicates that the experimentally determined deformation difference between these two configurations can only account for about 20% of the observed shifts in $\hbar\omega_c$. Such a result agrees with the expected small sensitivity of AB neutron band crossing frequency to deformations when the neutron Fermi level is close to the bottom of the $i_{13/2}$ subshell. The measured large shifts of crossing frequencies in decay sequences associated with the $h_{9/2} \frac{1}{2}^- [541]$ Nilsson configuration

versus other configurations for these nuclei are difficult to understand only in terms of deformation differences. A further theoretical investigation is needed to interpret the physical basis of this discrepancy.

4. Spectroscopic Phenomena at Higher Spin

4.1 Alignment Systematics above the AB Crossing

The systematics of the aligned angular momentum for the $N = 90$ isotones are summarized in fig.10. An interesting feature is observed in the negative-parity decay sequences of $^{161}\text{Lu}_{90}$, i.e. the gradual, yet sizable, alignment gain at intermediate frequencies ($0.25 < \hbar\omega < 0.40\text{MeV}$) between the neutron and proton band crossings, see fig.10. This feature is absent in the positive-parity decay sequences of ^{161}Lu , and the other odd- Z , $N = 90$ isotones. However, it is observed, though less pronounced, in the negative-parity decay sequences of $^{159}\text{Tm}_{90}$ and is nearly absent in the negative-parity decay sequences of $^{157}\text{Ho}_{90}$.

A similar gradual gain in alignment, increasing in magnitude as a function of Z , has been known ([Ric.1], [Ric.2] and [Fra.4]) at mid frequencies in the $(+,0)$ decay sequences of the even-mass, $N = 90$ isotones, see fig. 10. Since this feature is absent in the $(-,0)$, $(-,1)$, $(-, \frac{1}{2})$ and $(-, -\frac{1}{2})$ sequences (AF,AE, ABE, and ABF quasineutron excitations respectively) of the even- A , $N = 90$ and 91 isotones, it was suggested ([Ric.2] and [Fra.4]) to be the result of a band crossing associated with the excitation of the lowest-frequency pair of negative-parity quasineutrons (EF). This explanation, however, fails to explain the gradual alignments in the negative-parity decay sequences of $^{159}\text{Tm}_{90}$ and $^{161}\text{Lu}_{90}$, that are absent in the positive-parity sequences of these same nuclei. The positive- and negative-parity decay sequences in these odd- Z isotones should have the same quasineutron configuration: thus any quasineutron alignment should either occur, or not occur, in both positive- and negative-parity sequences. (These systematics are also discussed in refs. [Hüb.1] and [Bin.1]).

The physical basis of the relative alignment gains of the negative-parity decay sequences with respect to the positive-parity sequences in ^{159}Tm and ^{161}Lu remains unexplained. It is noted that this feature is more pronounced for nuclei with a smaller β_2 deformation and also is anti-correlated with the the stability of nuclear deformation in both the β_2 and γ degrees of freedom. No such gradual alignment

gains are observed for the heavier lutetium isotopes. This may be associated with a more stable nuclear shape for these isotopes resulting from the addition of neutrons. see also discussion in sect. 2.

4.2 Energy Signature Dependence above the AB Band Crossing

The large energy signature splittings at low spin (see subsect. 2.1), which favours the $\alpha = -\frac{1}{2}$ sequence, in the negative-parity decay sequences of the lighter lutetium isotopes and heavier $N = 90$ isotones disappears above the AB band crossings. see fig. 3. The small splitting above the AB band crossings for these nuclei favours the $\alpha = +\frac{1}{2}$ sequence. Such a dramatic change of signature splitting is the result of deformation changes due to the occupation of a pair of $i_{13/2}$ quasineutrons. The excited low- Ω $i_{13/2}$ quasineutron orbitals drive the nuclear shape toward a positive γ deformation, see the right-hand side of fig. 4, thus canceling the driving effect of quasiprotons ([Yu.1]), and producing a stable, axially-symmetric nuclear shape for these isotones and isotopes. It is noted that the relative change of energy signature splitting, $\Delta e'$, is the largest for ^{161}Lu , indicating a larger change of nuclear shape below and above the AB band crossing for this nucleus compared to the other isotones and isotopes. This feature is consistent with the "softness" of nuclear potential expected in this nucleus.

At the largest rotational frequencies, a sizable signature dependence of energy develops for ^{167}Lu in the negative-parity decay sequences based on the $\frac{3}{2}^- [514]$ Nilsson configuration, see fig. 3. A similar, though smaller, signature splitting in energy is also observed ([Fra.1] and [Fra.2]) for this configuration in ^{165}Lu , see fig. 3. Such a energy signature splitting at high spin is attributed to the admixture of the low- K $h_{11/2}$ components into the wave functions.

4.3 Transition Rates at Higher Spins

At the region of the $i_{13/2}$ quasineutron band crossing, the increases of the $B(M1)/B(E2)$ ratios for all the nuclei shown in fig. 7 are qualitatively expected in term of the increase in $B(M1)$ due to the increased neutron alignment. However, the magnitudes of the increases for the lighter lutetium isotopes are considerably larger than those for the other nuclei. Such a large increase can not be explained entirely by the increased $B(M1)$ values based on the experimental alignment gain if a stable, axially symmetric shape is assumed. The alignment gains associated with the AB neutron

band crossing for these isotonic and isotopic chains of nuclei have similar magnitudes. By assuming constant value of $B(E2)$, the relative increase of $B(M1)$ values at the band crossing can be extracted from the experimental ratios of $B(M1)/B(E2)$. Such experimentally extracted relative increases of $B(M1)$ values are compared with the "expected" increases according to eq.(2). Figure 11 shows such a comparison for $^{157}\text{Ho}_{90}$, $^{159}\text{Tm}_{90}$, and $^{161-167}\text{Lu}_{90-96}$. The experimental relative increases were obtained by assuming a constant value of $B(E2)$ and defined as:

$$\frac{B(M1, I \approx 20)}{B(M1, I \approx 10)} = \frac{\left(\frac{B(M1)}{B(E2)}\right)_{I \approx 20}}{\left(\frac{B(M1)}{B(E2)}\right)_{I \approx 10}} \quad (7)$$

where $\left(\frac{B(M1)}{B(E2)}\right)_{I \approx 20}$ and $\left(\frac{B(M1)}{B(E2)}\right)_{I \approx 10}$ are the averaged experimental $B(M1)/B(E2)$ ratios at spin $I \approx 20$ and $I \approx 10$ respectively. The expected relative increases of $B(M1)$ values are the ratios of the calculated $B(M1)$ values at $I = 20$ and $I = 10$ respectively. The proton and neutron gyromagnetic ratios used in the calculation are $g_p = 1.26$ and $g_n = -0.2$ for $h_{11/2}$ protons and $i_{13/2}$ neutrons. The effective g-factor for collective rotation, g_R , is assumed to be 0.4 below and 0.3 above the AB neutron band crossing. The alignment gains, Δi , caused by the excitation of a pair of $i_{13/2}$ quasineutrons, are taken from the experimental alignments.

The expected increase of $B(M1)$ values for ^{157}Ho , ^{159}Tm , ^{165}Lu and ^{167}Lu are in good agreement with the experimental values under the assumption of constant $B(E2)$ values. However, the expectations under-estimate the increases for ^{161}Lu and ^{163}Lu by a factor of 3 and 2 respectively. Such discrepancies can be the results of either an improper assumption of constant $B(E2)$ values or an abnormal behavior of $B(M1)$ values. Eq. (2) is valid only for nuclei with axially symmetric shape or small triaxiality ([Dön.1]). Both ^{161}Lu and ^{163}Lu are expected to have considerably large deviation from axial symmetry at low spin. For nuclei with large anisotropy ($|\gamma| \geq 20^\circ$) a difference in the principle moments of inertia should be considered ([Ham.2]). A different coupling scheme for the unfavoured states is also expected when $\gamma \approx -30^\circ$. In this coupling scheme the $B(M1)$ values are nearly quenched ([Ham.3]). Such a reduction of $B(M1)$ values due to the non-axial shapes below the AB band crossing gives rise to the relative increase of $B(M1)$ values at the crossing. A decrease of $B(E2)$ values can also enhance the relative increase of the $B(M1)/B(E2)$ ratios. The observed abnormally large increase of $B(M1)/B(E2)$ ratios at the AB

neutron band crossing most probably are the combination of a reduction of $B(M1)$ values below the band crossing due to the negative- γ deformation, and a decrease of $B(E2)$ values at the crossing.

An increase of $B(M1, I \rightarrow I - 1)/B(E2, I \rightarrow I - 2)$ ratios occurs at the largest spin for ^{150}Tm and ^{165}Lu , see fig. 7. Such an increase may be the result of a decrease of $B(E2)$ values. Detailed discussion for these increases are given refs. [Hag.2] and [Fra.2]. For ^{161}Lu , the $B(M1, I \rightarrow I - 1)/B(E2, I \rightarrow I - 2)$ ratios above the AB neutron band crossing remain the abnormally large value up to the rotational frequency where a proton alignment is expected to occur. Such a pattern suggests a possible decrease of $B(E2)$ values not only at the band crossing, as that discussed in the preceding paragraphs, but also at higher spins, since a decrease of $B(M1)$ value is expected due to the decrease of the effective K values as a function of $\hbar\omega$, see ref. [Dön.1]. At high angular momentum, a signature dependence of $B(M1)/B(E2)$ is observed in ^{167}Lu and ^{157}Ho . Such a signature dependence results from the rotationally induced Coriolis mixing that is also responsible for the signature splitting in energies (see the discussion in sects. 2.1, 2.2). The signature dependence of $B(M1, I \rightarrow I - 1)/B(E2, I \rightarrow I - 2)$ ratios in ^{167}Lu qualitatively agrees with the expectations from the signature dependence in energies.

5. Absolute Transition Probabilities

Direct information about nuclear shapes can be derived from the experimentally measured transition quadrupole moments. Such information is available for most of the $N = 90$ isotones. Figure 12 summarizes the transition quadrupole moments for the yrast bands of five $N = 90$ isotones. Two interesting features are observed when the odd- A nuclei are compared to their neighbouring even-even isotones: 1) The transition quadrupole moments for ^{157}Ho is smaller than ^{156}Dy and ^{160}Yb at low spin. 2) The decrease of Q_t as a function of spin exhibited in the even-even isotones is absent in both ^{157}Ho and ^{150}Tm .

The first feature suggests that ^{157}Ho has a smaller quadrupole deformation than its neighbouring even-even isotones. Two possible causes may be attributed to this odd-even deformation difference. The first cause may be the polarization of the nuclear shape by the odd proton which only exists in the odd- Z nucleus. The proton

$h_{11/2} \frac{7}{2}^- [523]$ orbit appears to be flat in the Nilsson diagrams (see the left-hand side of fig. 2). The cranked shell model calculation shows, however, this orbit has a driving force toward smaller quadruple deformations at a finite rotational frequency. The occupation of one such orbit in ^{157}Ho may have a stronger influence on the nuclear shape than the occupation of a pair of these orbits in ^{156}Dy and ^{160}Yb . Therefore ^{157}Ho exhibits a smaller quadruple deformation compared to ^{156}Dy and ^{160}Yb . The second cause may be associated with the different occupation probabilities of the proton $h_{9/2} \frac{1}{2}^- [541]$ orbit between the odd- Z and even-even isotones. The smaller proton pair correlations for the odd- Z nuclei indicates a smaller occupation probability of the $\frac{1}{2}^- [541]$ orbit, which is above, yet not too far away from the Fermi level for ^{157}Ho , ^{156}Dy , and ^{160}Yb . Since the $\frac{1}{2}^- [541]$ orbit has a strong driving force toward a large quadruple deformation, a smaller occupation probability of this orbit in ^{157}Ho naturally will produce a smaller quadruple deformation.

For ^{159}Tm , the Q_t values are nearly in between those of its neighbouring even-even isotones. This is hard to understand in term of the first cause of the odd-even deformation difference argued for ^{157}Ho , see the preceding paragraph. The second cause argued for ^{157}Ho , however, may not be valid for ^{159}Tm , since the $\frac{1}{2}^- [541]$ orbit is expected to be further away from the Fermi level for the heavier $N = 90$ isotones. It is therefore possible that no obvious odd-even deformation difference exists for the heavier $N = 90$ isotones.

The second odd-even difference, the absence of the decrease of Q_t as a function of spin for the odd- A isotones, may be partially associated with the odd-even deformation differences. The decrease of transition quadruple moments (or the $B(E2)$ values) as a function of spin were observed for the even-even $N = 90$ isotones ([Eml.1], [Osh.1], [Bec.1], and [Few.1]) and for several Yb isotopes ([Bac.2] and [Cla.1]). This phenomenon has been attributed ([Gar.1]) to the modification of single particle state by rotational motion. In the presence of rotationally-induced Coriolis and centrifugal forces, the degenerate pair of strongly polarizing nucleons (i.e. nucleons moving in a high- j , low Ω orbits), moving in time reversed orbits, becomes strongly split in energy. At a certain frequency, this splitting becomes large enough to cause the "unfavoured" state (corresponding to the nucleon moving in a direction opposite to the nuclear rotation) to be depopulated. The loss of such strongly shape-driving states below or

around the Fermi level causes the decrease of the nuclear quadruple deformation, thus resulting in a decrease of transition quadruple moment. A smaller quadruple deformation anticipated for ^{157}Ho (see the preceding paragraph) may cause the loss of the high-j, low- Ω orbit to occur at a much lower rotational frequency. For a smaller quadruple deformation, the neutron Fermi level is closer to the low- Ω components of the $i_{13/2}$ subshell. As a result, the nucleus does not need to rotate as fast to loose the anti-aligning, high-j orbit. Consequently no decrease of Q_t is observed for ^{157}Ho in the spin region where the decrease is observed for the even-even isotones (i.e. at or above the AB neutron band crossing, see fig. 12). For ^{157}Ho , the experimental Q_t decreases by 30% from spin 15/2 to 17/2 (see fig. 12). It should be noted, however, that at such a low spin, Q_t is sensitive to the effective K values used in the extraction of Q_t from the measured lifetime. The mixing of low-K components due to a small triaxiality expected in this nucleus may reduce the amount of the above mentioned decrease in Q_t . At higher spins, the Q_t values show no further decrease in ^{157}Ho . The connection between the lower-frequency (spin) occurrence of the decrease of Q_t and the smaller quadruple deformation is also observed in a systematic analysis ([Gar.2]) of this phenomenon for several Yb isotopes.

For ^{159}Tm , no obvious decrease of Q_t is observed even at low spin. Since ^{159}Tm has a larger quadruple deformation than ^{160}Yb (the Q_t values for ^{159}Tm are larger than those for ^{160}Yb at low spin; self-consistent calculation ([Wys.1]) also predicts a larger quadruple deformation for ^{159}Tm), the lack of decrease in ^{159}Tm compared to ^{160}Yb is difficult to understand in terms of the reasons argued for ^{157}Ho in the preceding paragraph. This indicates a more complicated mechanism behind the decrease of Q_t and the lack or earlier occurrence of this decrease in the odd-Z isotones. More data for the odd-Z nuclei are needed in order to fully understand this odd-even difference of transition quadruple moments.

6. Summary

Several recent high spin studies on the light lutetium isotopes, $^{161-167}\text{Lu}$ ([Yu.1], [Hon.1], [Jön.1], [Fra.1, 2] and [Yu.2]), and the odd-Z, $N = 90$ isotones, $^{157}\text{Ho}_{90}$, $^{159}\text{Tm}_{90}$, and $^{161}\text{Lu}_{90}$ ([Hag.1], [Gas.2], [Sim.1], [Gas.1], and [Yu.1]) are summarized and compared to the relevant even-even isotopes. The systematic analysis concentrates specially on the study of nuclear shapes and their stabilities for the odd-Z.

$N = 90$ isotones and the lutetium isotopes with respect to the various deformation degrees of freedom.

The results of the systematic analysis on energies and relative transition probabilities indicate that the heaviest lutetium isotope, ^{167}Lu , has not only the largest quadruple deformation but also the best defined shape with respect to the various deformation degrees of freedom. The nuclear shapes and other properties for the lighter isotopes can therefore be compared to such a good example of a well deformed light rare earth nucleus. The results from the comparison show evidences for a decreased quadruple deformation with decreasing neutron number for the lutetium isotopes and with increasing proton number for the $N = 90$ isotones. Energy signature splittings and their relations with the signature dependent transition rates at low spin indicate that the lightest lutetium isotope, ^{161}Lu has not only the smallest quadruple deformation, but also the least well defined shape among both the lutetium isotopes and $N = 90$ isotones. The "softness" of the nuclear potential is associated with both the quadruple deformation and the γ -degree of freedom. The neutron number dependence of shapes is consistent with the expectation in terms of the polarization effect of the valence particles. The low lying locations of the neutron Fermi levels in the neutron $i_{13/2}$ subshell for $^{161-169}\text{Lu}$ suggests a larger quadruple deformation and a more stable shape for a isotope occupying a larger number of low- Ω $i_{13/2}$ neutrons. Such a shape systematics is also consistent with the recently calculated equilibrium shapes at low spin for these isotopes. The same analysis carried out for the $N = 90$ isotones shows an opposite dependence of nuclear shapes on the proton number. The contrasting locations of the proton Fermi levels in the middle or upper portion of the $h_{11/2}$ proton subshell for the three odd- Z , $N = 90$ isotones result in an increased β_2 , γ deformation and shape stability for smaller number of protons.

The large signature splittings in energy at low spin and the incompatible relation of these splittings with the signature dependence of $B(M1)$ values expected for an axially symmetric system also suggest a significant triaxiality for the lighter lutetium isotopes and heavier $N = 90$ isotones. Such a deviation of nuclear shape from axial symmetry is understood as the result of the negative- γ driving force of the unpaired $h_{11/2}$ quasiproton. However, it is difficult to extract quantitative information about the γ deformation from the experimental data. The separation of static and dynamic

γ deformations is also difficult.

The polarization effects of different types of valence quasiprotons on the core shapes are studied by comparing the different configurations in the odd- Z , $N = 90$ isotones and lutetium isotopes. The yrast decay sequences of these nuclei are associated with the proton orbits lying in the middle or upper portion of the $h_{11/2}$ subshell. For the heavier lutetium isotopes and the lightest $N = 90$ isotone, $^{157}\text{Ho}_{90}$, level schemes are also established for the decay sequences associated with the $\frac{1}{2}^- [541]$ Nilsson state that lies at the bottom of the $h_{9/2}$ subshell. Comparisons of the quasineutron band crossing frequencies in the $\frac{1}{2}^- [541]$ band with those in the yrast configurations of their neighbouring even-even nuclei show significant differences. The systematic shifts of the AB quasineutron band crossing frequencies to a larger value in the $\frac{1}{2}^- [541]$ configuration than those in the other configurations are indicative of a larger quadruple deformation for this configuration. However, considerable discrepancies are observed between the expectations from the cranked shell model calculation based on the expected equilibrium deformations and the experimental data especially for the nuclei with neutron Fermi surface lying at the bottom of the $i_{13/2}$ subshell. A full understanding of the cause of the shift of the AB neutron band crossing calls for further investigation from the theoretical side.

Transition quadruple moments deduced from lifetime measurements for the $N = 90$ isotones are also presented and discussed in a systematic way. The smaller average value of the transition quadruple moments for $^{157}\text{Ho}_{90}$ extracted from the lifetime measurement compared to its neighbouring even-even isotones, ^{156}Dy and ^{158}Er , may be associated with the odd-even difference of proton pair correlations: the smaller proton pair correlations for ^{157}Ho gives a smaller occupation probability of the $\pi h_{9/2} \frac{1}{2}^- [541]$ configuration, making ^{157}Ho less driven to the large deformation by this orbit compared to its neighbouring even-even isotones. On the other hand, the presence of an odd proton in the $\pi h_{11/2} \frac{7}{2}^- [523]$ orbit in ^{157}Ho may drive the nucleus toward a smaller quadruple deformation. As a result, ^{157}Ho has a smaller quadruple deformation compared to its neighbouring even-even isotones. Although the lack of a decrease in Q_t at high spin for ^{157}Ho compared to the even-even isotones can be partially attributed to its smaller deformation (see sect. 5), the failure of interpreting the lack of decrease in ^{159}Tm using the same argument suggests a more complicated

mechanism behind this phenomenon.

Acknowledgments

The authors wish to thank I. Hamamoto, D. Radford, L.L. Riedinger and R. Wyss for valuable discussions during this work.

References

- And. 1 G. Andersson, S.E. Larsson, G. Leander, P. Möller, S.G. Nilsson, I. Ragnarsson, S. Åberg, R. Bengtsson, J. Dudek, B. Nerlo-Pomorska, K. Pomorski and Z. Szymański, Nucl. Phys. A268 (1976) 205.
- Bac. 1 J.C. Bacelar, M. Diebel, O. Andersen, J.D. Garrett, G.B. Hagemann, B. Herskind, J. Kownacki, C.-X. Yang, L. Carlén, J. Lyttkens, H. Ryde, W. Waluś and P.O. Tjøm, Phys. Lett. 152B (1985) 157
- Bac. 2 J.C. Bacelar, R.M. Diamond, E.M. Beck, M.A. Deleplanque, J. Draper, B. Herskind and F.S. Stephens, Phys. Rev. 35C (1987) 1170
- Bac. 3 J.C. Bacelar, R. Chapman, J.R. Leslie, J.C. Lisle, J.N. Mo, E. Paul, A. Simcock, J.C. Willmott, J.D. Garrett, G.B. Hagemann, B. Herskind, A. Holm, and P.M. Walker. Nucl. Phys. A442 (1985) 547
- Bar.1 R.A. Bark, G.D. Dracoulis, A.E. Stuchbery, A.P. Byrne, A.M. Baxter, F. Riess, and P.K. Weng, J. Phys. G: 15 (1989) L169
- Bec. 1 E.M. Beck, H. Hübel, R.M. Diamond, J.C. Bacelar, M.A. Deleplanque, K.H. Meier, R.J. McDonald, F.S. Stephens and P.O. Tjøm. Phys. Lett. 215B (1988) 624.
- Ben. 1 R. Bengtsson, H. Frisk, F.R. May and J.A. Pinston. Nucl. Phys. A415 (1984) 189
- Ben. 2 R. Bengtsson, J. de Physique (Coll.) C10 (1980) 87; and S.G. Nilsson and C.F. Tsang, Nucl. Phys. A131 (1969) 1
- Ben. 3 T. Bengtsson and I. Ragnarsson. Nucl. Phys. A436 (1985) 14.

- Bin. 1 C.R. Bingham, L.L. Riedinger, L.H. Courtney, Z.M. Liu, A.J. Larabee, M. Craycraft, D.J.G. Love, P.J. Nolan, A. Kirwan, D.J. Thornley, P.J. Bishop, A.H. Nelson, M.A. Riley and J.C. Waddington, *J. Phys. G* 14 (1988) L77.
- Boh. 1 Aa. Bohr and B. Mottelson, *Nuclear Structure* (Benjamin, Vol. 1 (1969) and Vol. 2 (1975), reading).
- Cla. 1 D. Clarke, R. Chapman, F. Khazaie, J.C. Lisle, J.N. Mo, K. Schiffer, J.D. Garrett, G.B. Hagemann, B. Herskind, K. Theine, W. Schmitz, and H. Hübel. *Manchester Annual Report*, (1989) 72.
- Dön. 1 F. Dönau, *Nucl. Phys.* A471 (1987) 469.
- Eml. 1 H. Emling, I. Ahmad, P.J. Daly, B.K. Dichter, M. Drigert, U. Garg, Z.W. Grabowski, R. Holzmann, R.V.F. Janssens, T.L. Khoo, W.C. Ma, M. Piipariinen, M.A. Quader, I.Ragnarsson and W.H. Trzaska, *Phys. Lett.* 217B (1989) 33.
- Few. 1 M.P. Fewell, N.R. Johnson, F.K. McGowan, J.S. Hattula, I.Y. Lee, C. Baktash, Y. Schutz, J.C. Wells, L.L. Riedinger, M.W. Guidry and S.C. Pancholi, *Phys. Rev. Lett.* 37 (1988) 101
- Fra. 1 P. Frandsen, J.D. Garrett, G.B. Hagemann, B. Herskind, M.A. Riley, R. Chapman, J.C. Lisle, J.N. Mo, L. Carlén, J. Lyttkens, H. Ryde and P.M. Walker, *Phys. Lett.* B177 (1986) 287
- Fra. 2 P. Frandsen, R. Chapman, J.D. Garrett, G.B. Hagemann, B. Herskind, C.-H. Yu, K. Schiffer, D. Clarke, F. Khazaie, J.C. Lisle, J.N. Mo, L. Carlén, P. Ekström and H. Ryde, *Nucl. Phys.* A489 (1988) 503
- Fra. 3 S. Frauendorf and F.R. May, *Phys. Lett.* 105B (1981) 5.
- Fra. 4 S. Frauendorf, L.L. Riedinger, J.D. Garrett, J.J. Gaardhoje, G.B. Hagemann and B. Herskind, *Nucl. Phys.* A431 (1984) 511.
- Gaa. 1 J.J. Gaardhoje. Thesis, Univ. of Copenhagen. 1980.

- Gar. 1 J.D. Garrett, J. Nyberg, C.-H. Yu, J.M. Espino and M.J. Godfrey, in *Contemporary Topics in Nuclear Structure Physics*, ed. R.F. Casten. et al. (World Scientific, 1988, Singapore) p.699.
- Gar. 2 J.D. Garrett, contribution to the Workshop on Nuclear Structure at High Spins. Bad Honnef, Germany, March, 1989. P.100.
- Gas. 1 J. Gascon, P. Taras, D.C. Radford, D. Ward, H.R. Andrews and F. Banville. *Nucl. Phys. A467* (1987) 539.
- Gas. 2 J. Gascon, C.-H. Yu, G.B. Hagemann, M.C. Carpenter, J.M. Espino, Y. Iwata, T. Kamatsubara, J. Nyberg, S. Ogaza, G. Sletten, P.O. Tjøm, D.C. Radford, J. Simpson, M.A. Bentley, P. Fallon, P.D. Forsyth and J.F. Sharpey-Schafer, to be published.
- Hag. 1 G.B. Hagemann, J.D. Garrett, B. Herskind, J. Kownacki, B.M. Nyakó, P.L. Nolan, J.F. Sharpey-Schafer and P.O. Tjøm, *Nucl. Phys. A424* (1984) 365
- Hag. 2 G.B. Hagemann, R. Chapman, P. Frandsen, A.R. Mokhtar, M. Riley, J. Simpson and C.-H. Yu, in *Proc. of Int. Conf. on Nuclear Structure Through Static and Dynamic Moments*, Melbourne, Australia, Aug. 1987. p.313.
- Hag. 3 G.B. Hagemann and I. Hamamoto, preprint "Lund-MPH-89/04" and to be published.
- Ham. 1 I. Hamamoto and H. Sagawa, *Phys. Lett. B201* (1988) 415.
- Ham. 2 I. Hamamoto in *Nuclear Structure*. Proc. of Niels Bohr Centennial Conf. eds. R. Broglia, G.B. Hagemann and B. Herskind. (North Holland, 1985. Amsterdam) p.129.
- Ham. 3 I. Hamamoto. *Phys. Lett. B193* (1987) 399.
- Har. 1 S.M. Harris. *Phys. Rev. 138* (1965) B509
- Hon. 1 K. Honkanen, H.C. Griffin, D.G. Sarantites, V. Abenante, L.A. Adler, C. Bakdash, Y.S. Chen, O. Dietzsch, M.L. Halbert, D.C. Hensley, N.R. Johnson, A.J. Larabee, I.Y. Lee, L.L. Riedinger, J.X. Saladin, T.M. Semkow and Y. Schutz.

in ACS Symposium Series No.324, Nuclei off the Line of Stability. ed. R.A. Meyer and D.S. Brenner, 1986, American Chemical Society. p.317

- Hüb. 1 H. Hübel, M. Murzel, E.M. Beck, H. Kluge, A. Kuhnert, K.H. Maier, J.C. Bacelar, M.A. Deleplanque, R.M. Diamond and F.S. Stephens, *Z. Phys. A* 329 (1988) 289
- Jön. 1 S. Jönsson, J.Lyttkens, L. Carlén, N. Roy, H. Ryde, W. Waluś, J.Kownacki, G.B. Hagemann, B. Herskind, J.D. Garrett and P.O. Tjøm, *Nucl. Phys. A*422 (1984) 397
- Jön. 2 S. Jönsson, N. Roy, H. Ryde, W. Waluś, J. Kownacki, J.D. Garrett, G.B. Hagemann, B. Herskind, R. Bengtsson and S. Åberg, *Nucl. Phys. A*449 (1986) 537
- Kow. 1 J. Kownacki, J.D. Garrett, J.J. Gaardhoje, G.B. Hagemann, B. Herskind, S. Jonsson, N. Roy, H. Ryde and W. Waluś, *Nucl.Phys. A*394 (1983) 269
- Lar. 1 A.J. Larabee and J.C. Waddington, *Phys. Rev. C*24 (1981) 2367
- Lar. 2 A.J. Larabee L.H. Courtney, S. Frauendorf, L.L. Riedinger, J.C. Waddington, M.P.Fewell, N.R. Johnson, I.Y. Lee and F.K. McGowan, *Phys. Rev. C*29 (1984) 1934
- Lea. 1 G.A. Leander, S. Frauendorf and F.R. May, in *Proceedings of the Conference on High Angular Momentum Properties of Nuclei*, Oak Ridge, 1982, p.281.
- Li.1 S.G. Li, C.-X. Yang, R. Chapman, F. Khazaie, J.C. Lislie, J.N. Mo, J.D. Garrett, G.B. Hagemann, B. Herskind and H. Ryde, *Manchester Annual Report* (1987) p.52. and G.-J. Yuan, G.-S. Li, S.-X. Wen, S.-G. Li, P.-F. Hua, L. Zhou, P. Wu, L.-K. Zhang, Z.-K. Yu, P.-S. Yu, P.-K. Wen and C.-X. Yang, *Chinese Journal of Nuclear Physics*, 11 (1989) 1
- Naz. 1 W. Nazarewicz, J. Dudek, R. Bengtsson, T. Bengtsson and I. Ragnarsson, *Nucl. Phys. A*435 (1985) 397.

- Naz. 2 W. Nazarewicz, M.A. Riley, J.D. Garrett and J. Dudek, Proceedings of the International Conference on Nuclear Shapes. Crete, 1987, p.67 and to be published
- Osh. 1 M. Oshima, N.R. Johnson, F.R. McGowan, C. Baktash, I.Y. Lee, Y. Schutz, R.V. Ribas and J.C. Wells, Phys. Rev. C33 (1986) 1988.
- Rad. 1 D. Radford, in Contribution to the Workshop on Nuclear Structure. The Niels Bohr Institute, May, 1988; and D.C. Radford, H.R. Andrews, D. Horn, D. Ward, F. Banville, S. Flibotte, P. Taras, J. Johansen, D. Tucker and J.D. Waddington. in press.
- Rie. 1 L.L. Riedinger, O.Andersen, S. Frauendorf, J.D. Garrett, J.J. Gaardhoje, G.B. Hagemann, B. Herskind, Y.V. Makovetzky, J.C. Waddington, M. Guttormsen and P.O. Tjøm, Phys. Rev. Lett. 44 (1980) 568.
- Rie. 2 L.L. Riedinger, Phys. Scr. T5 (1983) 36
- Sim. 1 J. Simpson, B.M. Nyakó, A.R. Mokhtar, M. Bentley, H.W. Cranmer-Gordon, P.D. Forsyth, J.D. Morrison, J.F. Sharpey-Schafer, M.A. Riley, J.D. Garrett, C.-H. Yu, A. Johnson, J. Nyberg and R. Wyss, in Proceedings of the International Nuclear Physics Conference, Harrogate, U.K. Aug. 1986. Vol.1, p.B66, and to be published.
- Sim. 2 J. Simpson, D.V. Elenkov, P.D. Forsyth, D. Howe, B.M. Nyakó, M.A. Riley, J.F. Sharpey-Schafer, B. Herskind, A. Holm, and P.O. Tjøm, J. Phys. G, 12 (1986) L67.
- Sim.3 J. Simpson, M.A. Riley, J.R. Crosswell, P.D. Forsyth, D. Howe, B.M. Nyakó, J.F. Sharpey-Schafer, J. Bacelar, J.D. Garrett, G.B. Hagemann, B. Herskind and A.Holm. Phys. Rev. Lett. 53(1984) 648
- Tjo. 1 P.O. Tjøm, R.M. Diamond, J.C. Bacelar, E.M. Beck, M.A. Deleplanque, J.E. Draper and F.S. Stephen. Phys. Rev. Lett. 55 (1985) 2405
- Wal. 1 W. Waluś, N. Roy, S. Jönsson, L.Carlén, H. Ryde, J.D. Garrett, G.B. Hagemann, B. Herskind, Y.S. Chen, J. Alnberger and G. Leader, Phys. Scripta 24 (1981) 324

- Wal.2 W. Waluś, L. Carlén, S. Jönsson, J. Lyttkens, H. Ryde, J. Kownacki, W. Nazarewicz, J.C. Bacelar, J. Dudek, J.D. Garrett, G.B. Hagemann, B. Herskind and C.-X. Yang, *Phys. Scr.* 34 (1986) 710
- Wys.1 R. Wyss, R. Bengtsson, W. Nazarewicz and J. Nyberg. private communication and to be published
- Yu. 1 C.-H. Yu, M.A. Riley, J.D. Garrett, G.B. Hagemann, J. Simpson, P.D. Forsyth, A. R. Mokhtar, J. D. Morrison, B. M. Nyakó, J.F. Sharpey-Shafer and R. Wyss, *Nucl. Phys. A*489 (1988) 477.
- Yu. 2 C.-H. Yu, G.B. Hagemann, J.M Espino, K. Furuno, J.D. Garrett, R. Chapman, D. Clarke, F. Khazaie, J.C. Lisle, J.N. Mo M. Bergström, L. Carlén, P. Ekström, J. Lyttkens and H. Ryde, to be published in *Nucl. Phys. A*.

Figure Captions

Figure 1: The $N = 90$ isotones and odd- A lutetium isotopes discussed in this work.

Figure 2: Nilsson-model diagrams (plots of single-particle energy as a function of quadruple deformation, ϵ) for protons (left-hand side) and neutrons (right-hand side) calculated using modified-oscillator potentials ([Ben.2]) parametrized as in ref. [Ben.3].

Figure 3: Energy signature splitting, $\Delta\epsilon' \equiv \epsilon'(\alpha = +1/2) - \epsilon'(\alpha = -1/2)$, as a function of rotational frequency for the decay sequences associated with the proton $h_{11/2}$ yrast configurations in $^{161-167}\text{Lu}$, ^{157}Ho and ^{159}Tm . See sect. 1 for data sources.

Figure 4: Cranked shell model calculation of the γ -dependence of the lowest negative-parity quasiproton (left-hand portion) and positive-parity quasineutron (right-hand portion) configurations at $\hbar\omega = 0.03 \hbar\omega_0$ (0.23 MeV). Solid and dashed curves denote $\alpha = +\frac{1}{2}$ and $\alpha = -\frac{1}{2}$ respectively. The proton and neutron Fermi levels [$\lambda_p = 5.88\hbar\omega_0$ (For ^{161}Lu , $\hbar\omega_0 = 7.240$ and 7.833 MeV for protons and neutrons respectively), $\lambda_n = 6.46\hbar\omega_0$] were fixed at $\gamma = 0$ to correspond to $Z = 71$ and $N = 90$. The deformation parameters, $\epsilon_2 = 0.2$ and $\epsilon_4 = 0$, are appropriate for $^{161}\text{Lu}_{90}$. The pair gap parameter, Δ , was taken to be $0.14 \hbar\omega_0$ ($= 1.05$ MeV), i.e. approximately equal to 80% and 90% of the odd-even mass differences for protons and neutrons respectively. The remaining parameters of the oscillator potential were taken from ref. [Ben. 3].

Figure 5: Comparison of the prolate and oblate orbitals in prolately-deformed nuclei. The intrinsic angular momentum, j , for nucleons moving in such orbitals are indicated together with the projections on the nuclear symmetry axis, Ω , and on the axis of rotation, j_r .

Figure 6: Comparison of calculated ([Wys.1]) potential energy surfaces for the lowest negative-parity, $\alpha = -1/2$ configurations of $^{161,163,165,167}\text{Lu}$, ^{157}Ho and ^{159}Tm . These surfaces were calculated as a function of β_2 and γ at $\hbar\omega \approx 0.2$ MeV using the Nilsson Strutinsky procedure. The pairing gap parameters are fixed at the values calculated with the BCS method at $\hbar\omega = 0$.

Figure 7: $B(M1, I \rightarrow I - 1)/B(E2, I \rightarrow I - 2)$ ratios as a function of spin for $^{157}\text{Ho}_{90}$, $^{159}\text{Tm}_{90}$, and $^{161-167}\text{Lu}_{90-96}$. See sect. 1 for data sources. For ^{159}Tm the ratio corresponding to $I = 33.5\hbar$ is 3.25 ± 0.03 .

Figure 8: Comparison of “expected” [see eq. (4)] and experimentally extracted relative B(M1) signature splittings averaged at spin $\approx \frac{19}{2}$ for the yrast configuration of $^{157}\text{Ho}_{90}$, $^{159}\text{Tm}_{90}$, and $^{161-167}\text{Lu}_{90-96}$.

Figure 9: Summary of the shifts, $\delta\hbar\omega_c$, of the AB quasineutron band crossing frequencies, for the decay sequences based on the $\frac{1}{2}^- [541]$ Nilsson configuration in ^{157}Ho ([Rad.1], ^{165}Lu ([Jön. 1] and [Fra. 1]), ^{167}Lu ([Yn.2]), ^{169}Ta [(Li.1)], $^{171,173}\text{Ta}$ ([Bac.3]), ^{171}Re ([Bar.1]), and ^{177}Re ([Wal.2]) with respect to this crossing in the neighbouring even-even isotones. The precise definition of $\delta\hbar\omega_c$ is given in eq. (5).

Figure 10: Comparison of the experimental alignments for selected decay sequences of the $N = 90$ isotones (see sect. 1 for data sources). All the values are referred to a reference configuration parametrized by the Harris formula, $J = J^{(0)} + J^{(1)}\omega^2$ ([Har.1]) with $J^{(0)} = 29\text{MeV}^{-1}\hbar^2$ and $J^{(1)} = 32\text{MeV}^{-3}\hbar^4$.

Figure 11. Comparison of experimental (solid points) and predicted (open points) relative increase of the B(M1) values due to the excitation of a pair of $i_{13/2}$ quasineutrons for decay sequences associated with the high-K proton $h_{11/2}$ Nilsson state in $^{161,163,165,167}\text{Lu}$, ^{157}Ho and ^{159}Tm . The empirically predicted relative increases were calculated using Dönau’s formula, eq. (2), and the experimental alignment gains at the band crossing, see text.

Figure 12: Experimental quadrupole moments for the $\Delta I = 2$ transitions in the yrast decay sequences of $^{156}\text{Dy}_{90}$, $^{157}\text{Ho}_{90}$, $^{158}\text{Er}_{90}$, $^{159}\text{Tm}_{90}$, and $^{160}\text{Yb}_{90}$. Data are taken from [Eml.1], [Hag.1], [Gas.2], [Osh.1], [Bec.1], [Gas.1] and [Few.1].

DISCLAIMER

This report was prepared as an account of work sponsored by an agency of the United States Government. Neither the United States Government nor any agency thereof, nor any of their employees, makes any warranty, express or implied, or assumes any legal liability or responsibility for the accuracy, completeness, or usefulness of any information, apparatus, product, or process disclosed, or represents that its use would not infringe privately owned rights. Reference herein to any specific commercial product, process, or service by trade name, trademark, manufacturer, or otherwise does not necessarily constitute or imply its endorsement, recommendation, or favoring by the United States Government or any agency thereof. The views and opinions of authors expressed herein do not necessarily state or reflect those of the United States Government or any agency thereof.

Neutron Number N

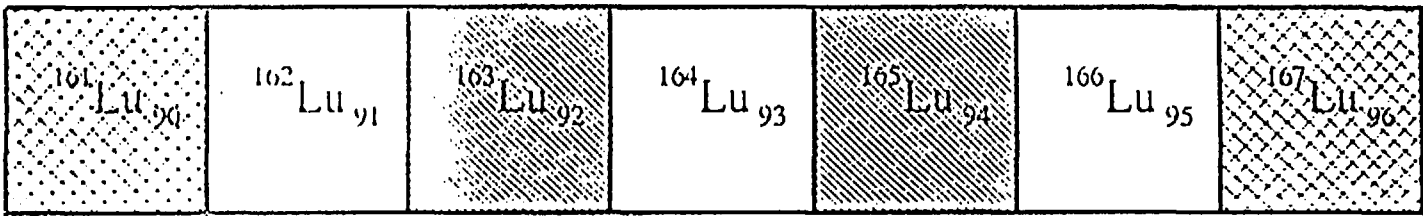
90

92

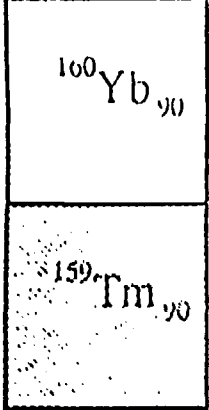
94

96

71



69



67

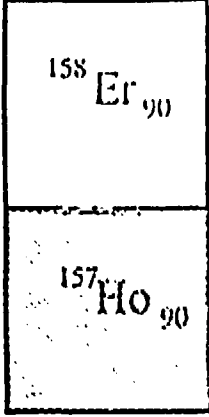


Fig. 1

figure 1.

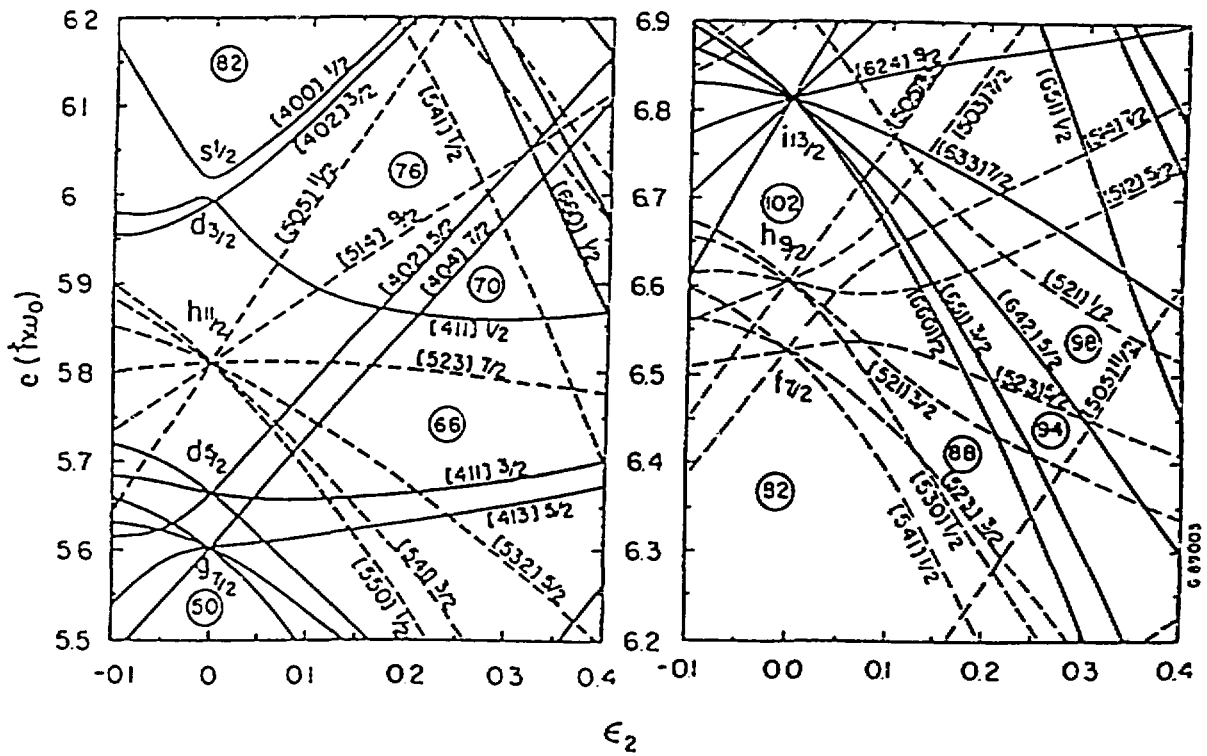


Fig. 1

Fig. 2

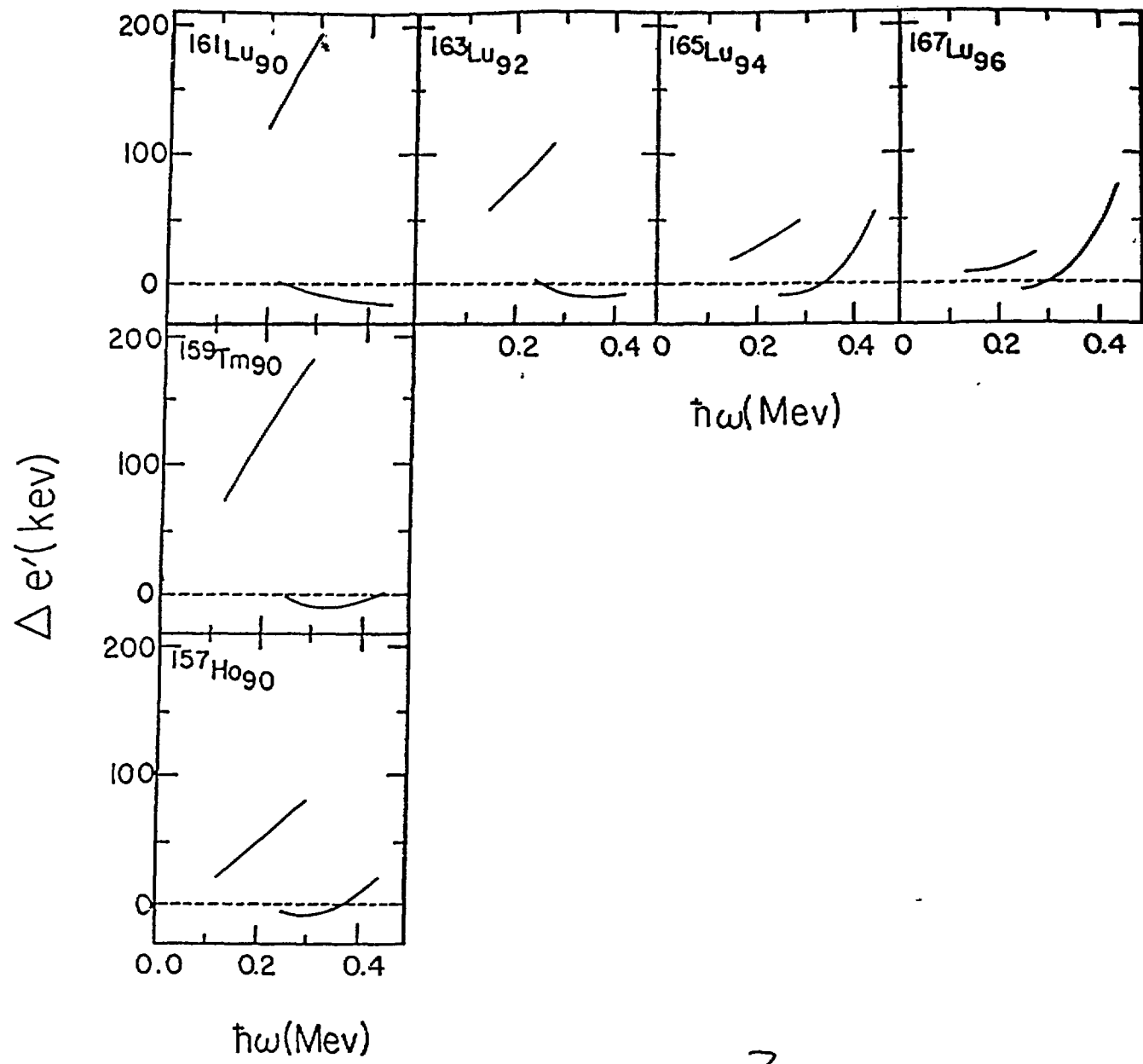


Fig. 3

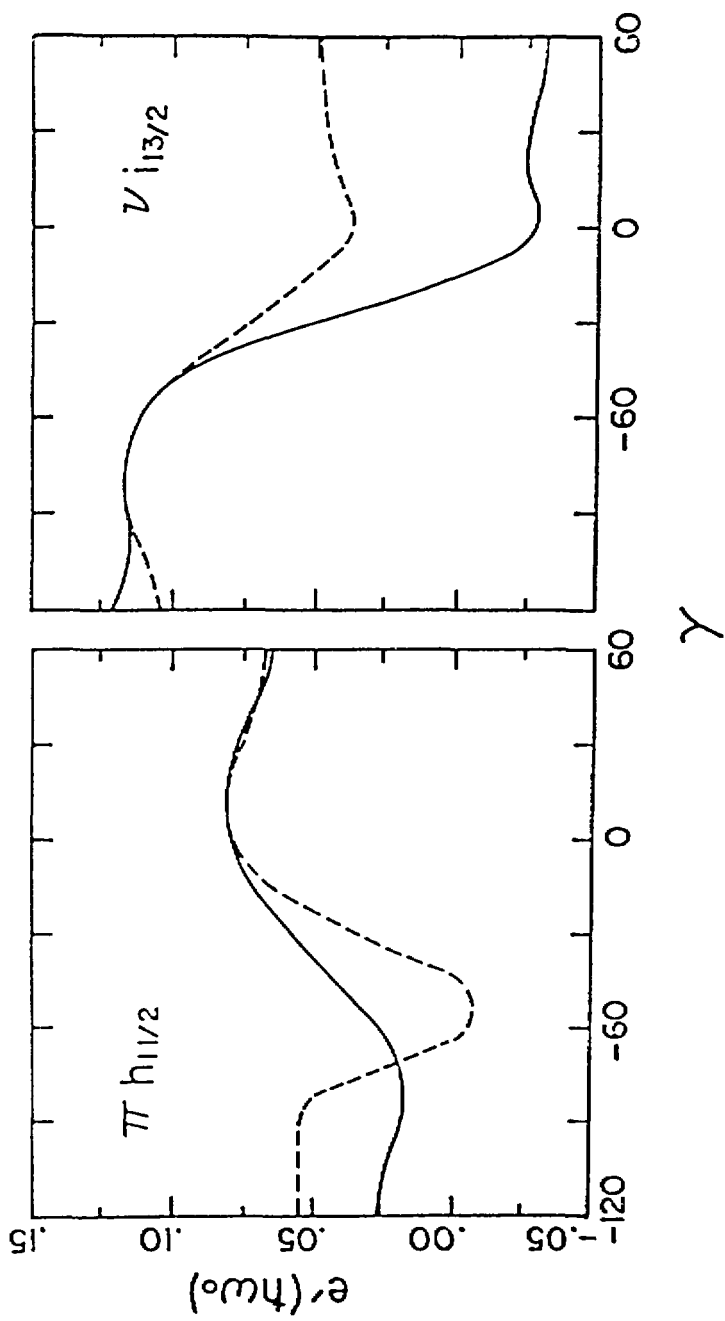
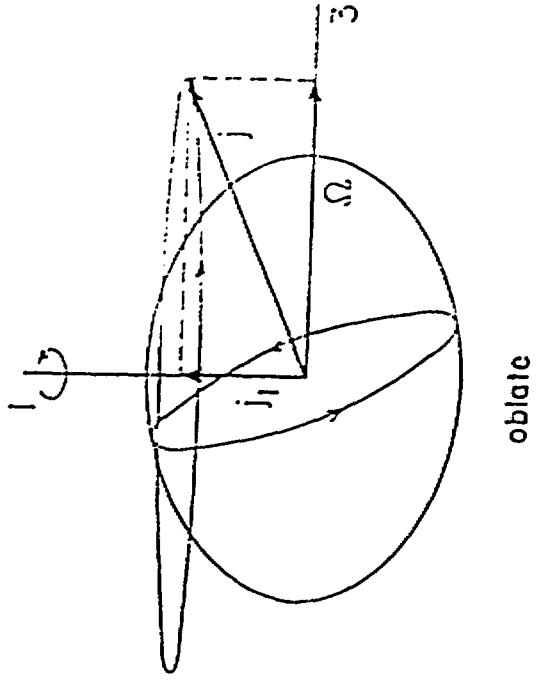
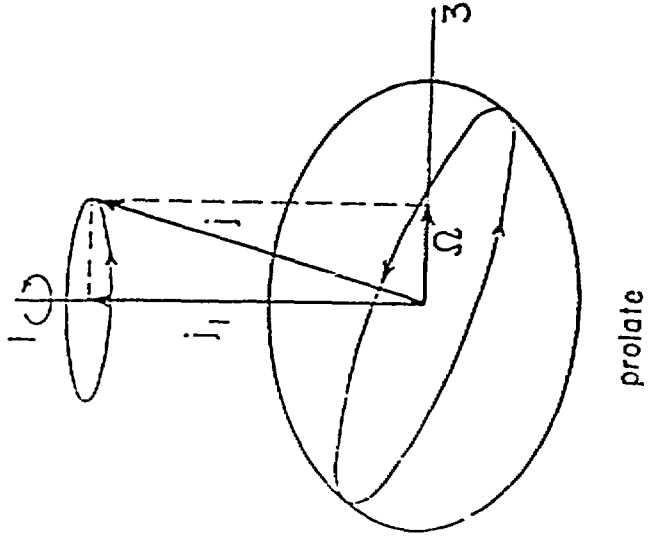
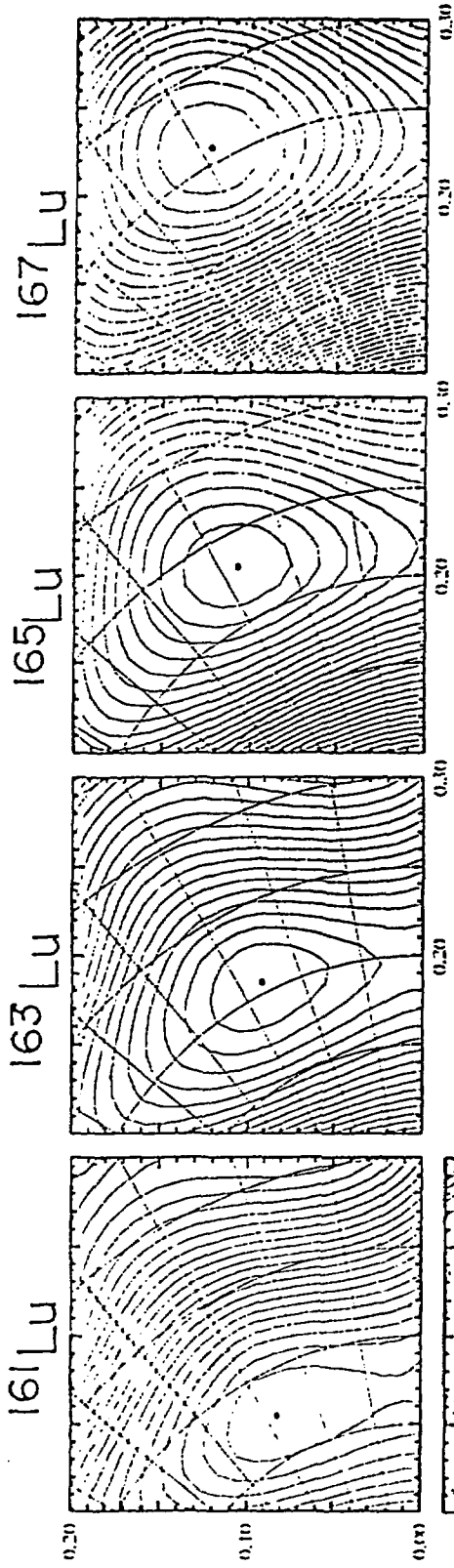


Fig 4
Figure 4

Figure 5
Fig. 5

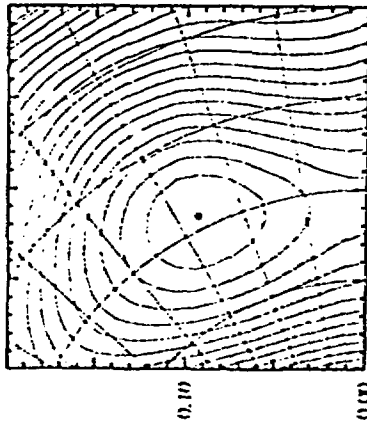




$$Y = \beta_2 \sin(\gamma + 30^\circ)$$

$$X = \beta_2 \cos(\gamma + 30^\circ)$$

159 Tm



157 Ho

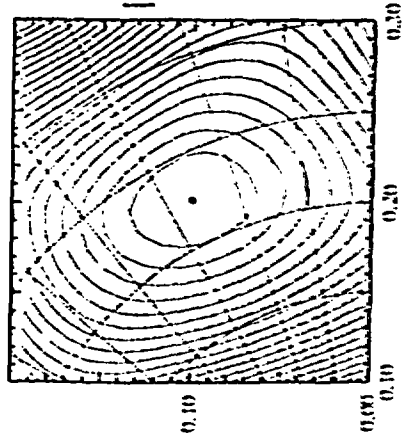
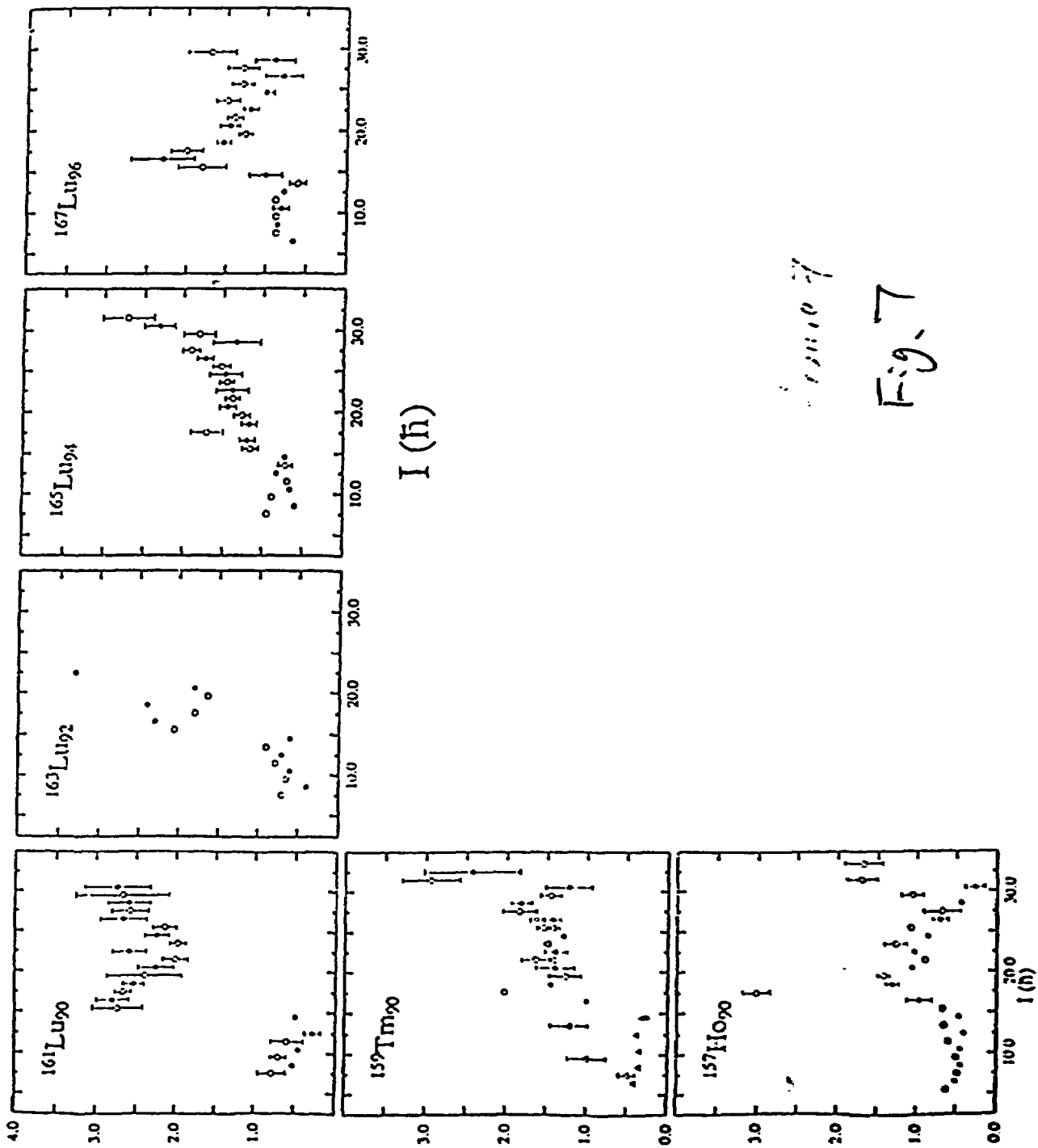


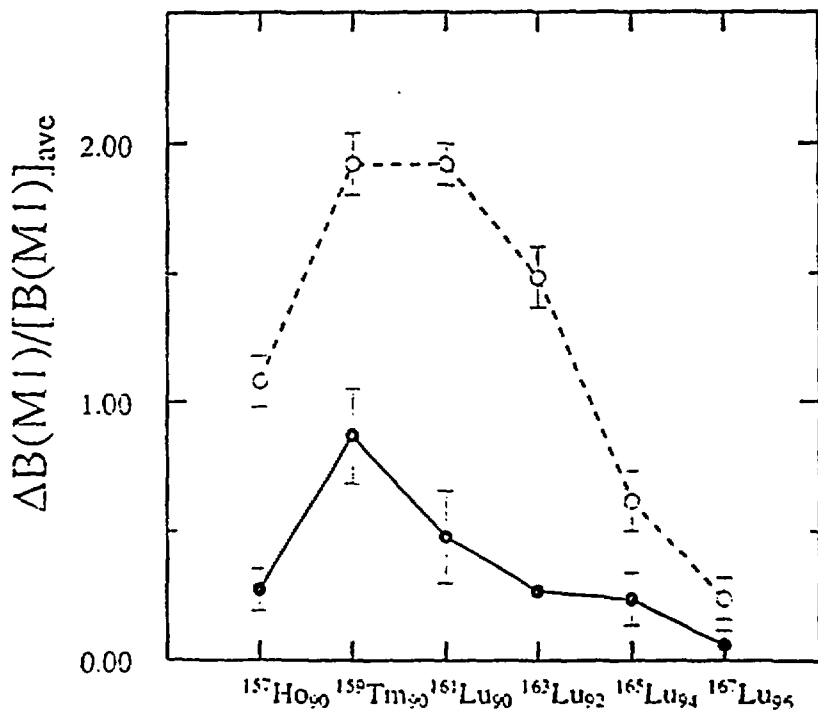
Fig. 6

Figure 6



12007
Fig. 7

Figure 8



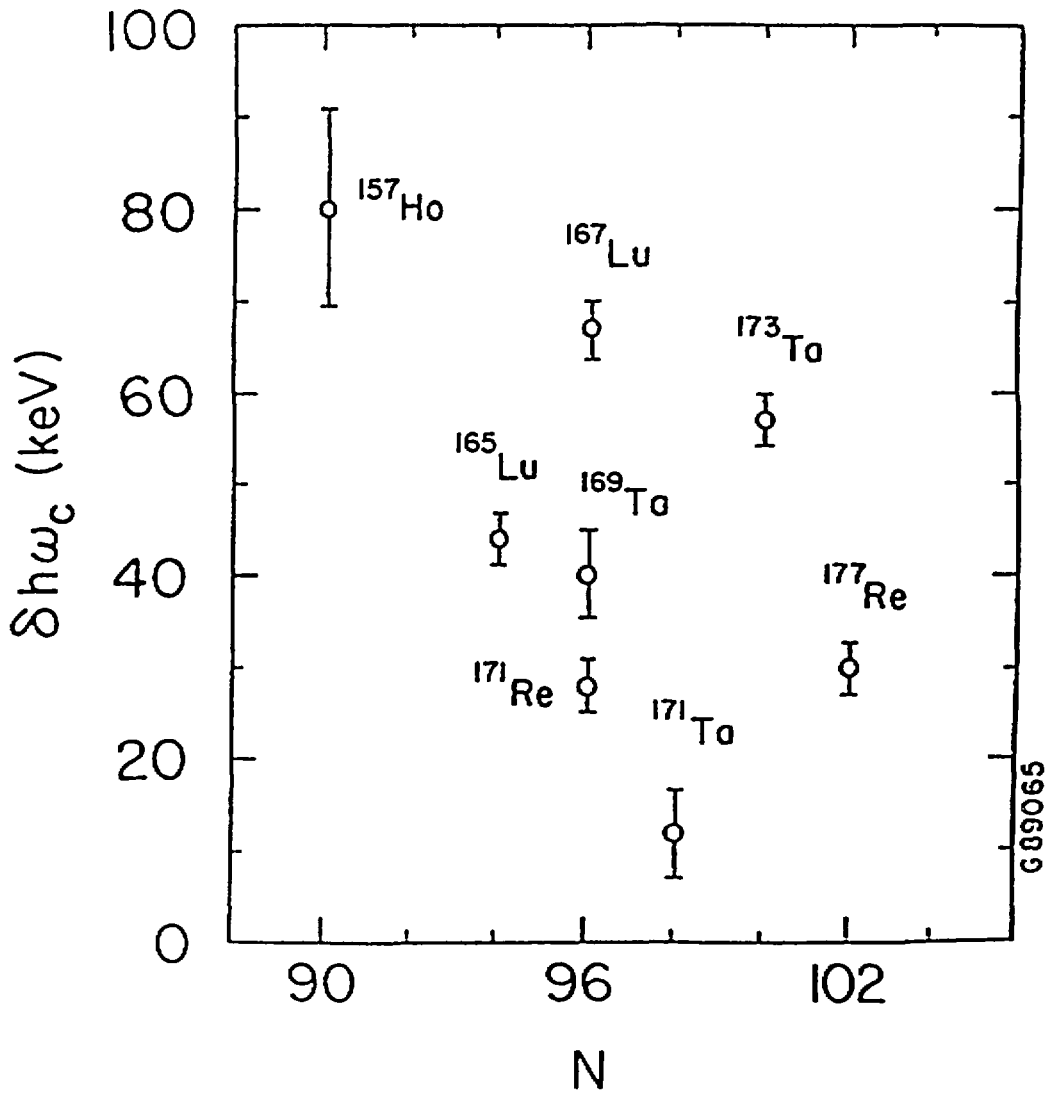


Fig. 9

689065

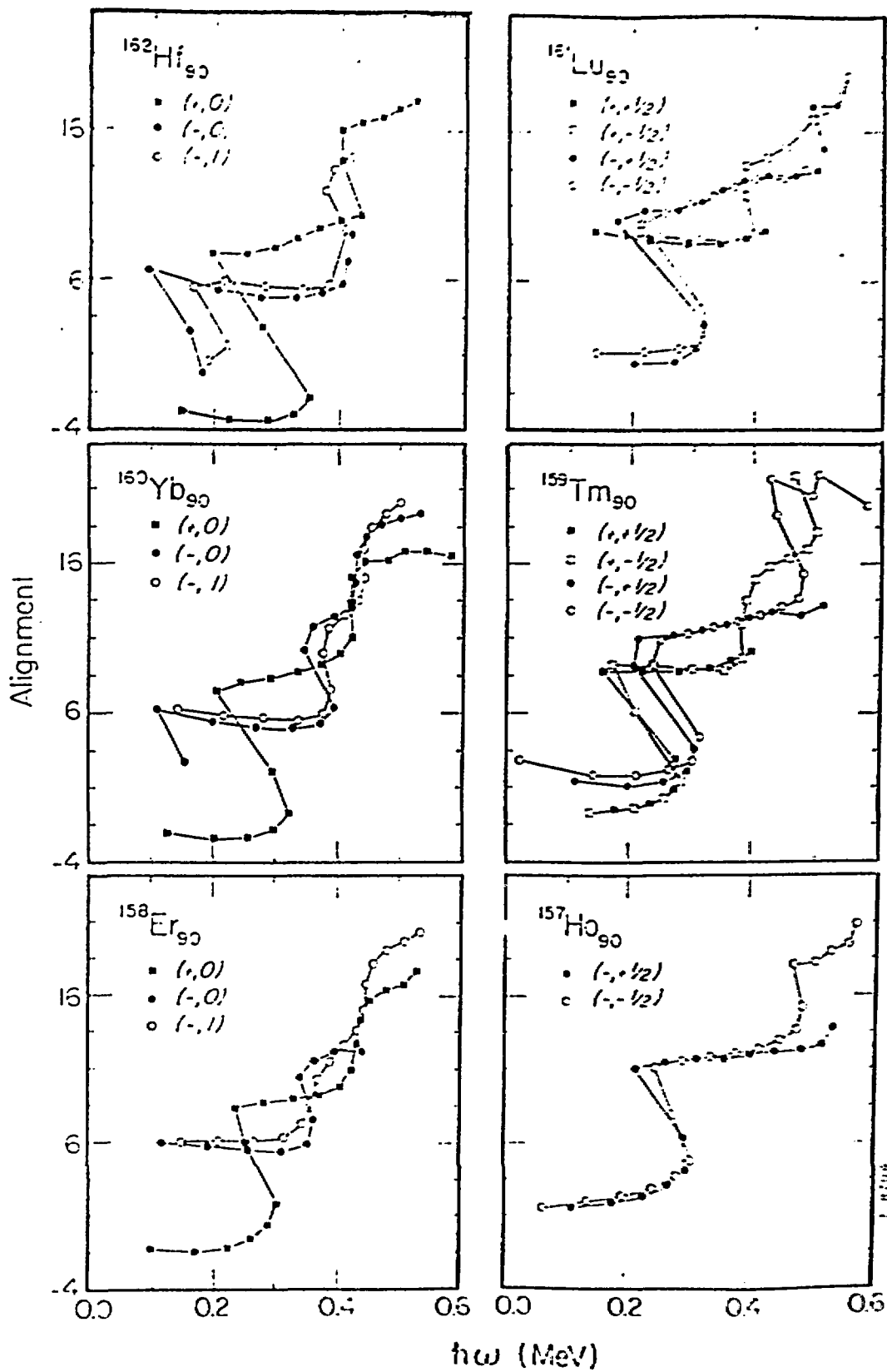
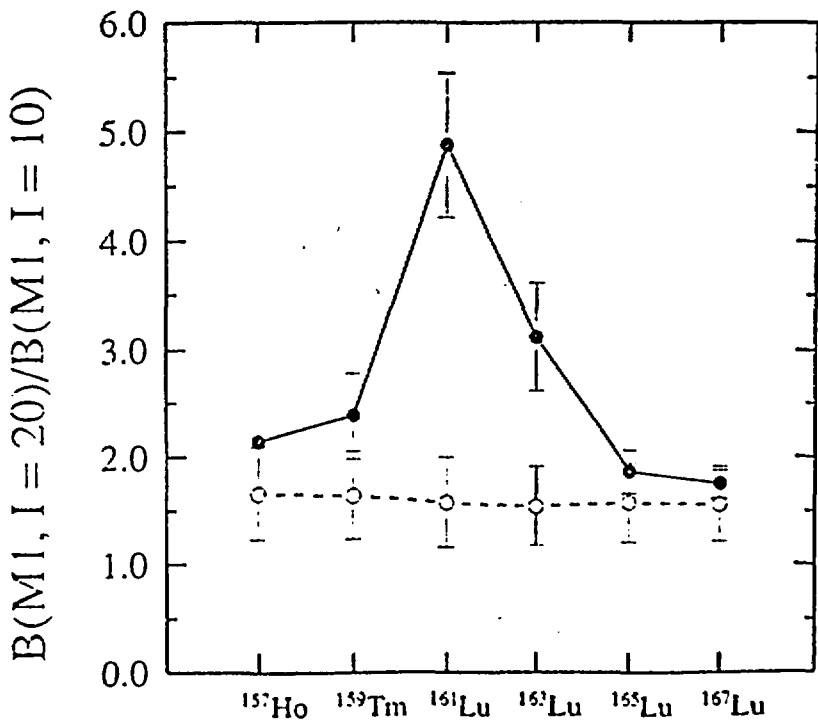
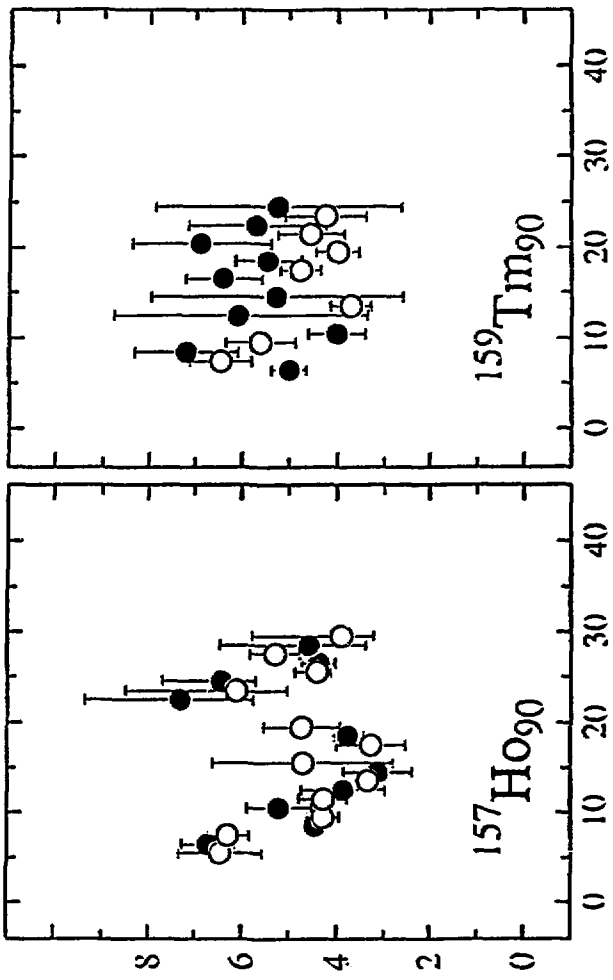
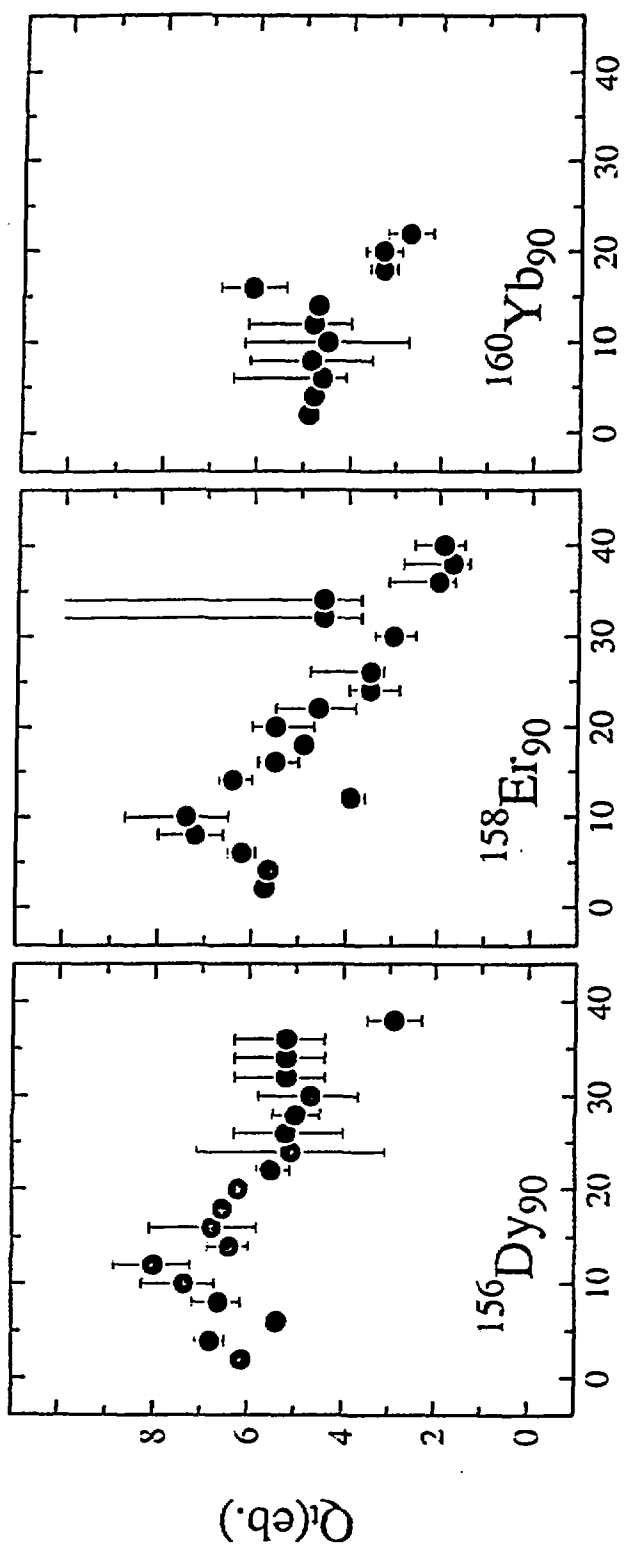


figure 10

Figure 11





Spin (h)

Figure 12